RM No. E6L04

NACA

RESEARCH MEMORANDUM

for the

Bureau of Aeronautics, Navy Department

PERFORMANCE OF THE 19XB 10-STAGE AXIAL-FLOW COMPRESSOR

By Richard M. Downing and Harold B. Finger

Aircraft Engine Research Laboratory
Cleveland, Ohio

NATIONAL ADVISORY COMMITTEE FOR AERONAUTICS

WASHINGTON

NACA RM No. E6L04

NATIONAL ADVISORY COMMITTEE FOR AERONAUTICS

RESEARCH MEMORANDUM

for the

Bureau of Aeronautics, Navy Department

PERFORMANCE OF THE 19XB 10-STAGE AXIAL-FLOW COMPRESSOR

By Richard M. Downing and Harold B. Finger

SUMMARY

An investigation has been conducted to determine the performance characteristics of the 10-stage axial-flow compressor for the 19XB jet-propulsion engine. Initial performance data were taken with inlet conditions of 59° F and 14 inches of mercury absolute over a range of speeds from 3400 to 17,000 rpm with interstage instruments installed and with normal air leakage past the rotor rear air seal. The effects of interstage instruments, of air leakage past the rotor rear air seal, and of inlet air conditions were then separately evaluated.

At the design speed of 17,000 rpm the compressor had a peak adiabatic temperature-rise efficiency of 0.72 and developed a pressure ratio of 3.72 at a weight flow of 33.8 pounds per second. A maximum efficiency of 0.75 was obtained at the equivalent speed of 15,300 rpm.

The removal of the interstage instruments increased the weight flow 2.2 percent and the peak temperature-rise efficiency 0.03 at the design speed. The elimination of the air leakage past the rotor rear air seal at the design speed decreased the peak adiabatic temperature-rise efficiency 0.04, decreased the equivalent weight flow 5 percent, and increased the peak pressure ratio 0.25. A change in the inlet conditions from 59° F and 14 inches of mercury absolute to -59° F and 6.5 inches of mercury absolute increased the peak pressure ratio at design speed 0.74 and decreased the weight flow by approximately 6 percent. The results of the surveys with the interstage instruments located in each stator row and the first row of outlet guide vanes indicated that some nonuniformity of blade loading existed and that a considerable loss of total pressure was occasioned by the outlet guide vanes.

INTRODUCTION

The 19XB compressor, which replaces the 19B compressor (reference 1) and has the same length and diameter as the 19B compressor, was designed with 10 stages to deliver 30 pounds of air per second for a pressure ratio of 4.17 at an equivalent speed of 17,000 rpm; the 19B was designed with six stages for a pressure ratio of 2.7 at the same weight flow and speed as the 19XB compressor. The performance characteristics of the new compressor were determined at the NACA Cleveland laboratory at the request of the Bureau of Aeronautics, Navy Department.

Results are presented of the investigation made to evaluate the over-all performance of the compressor, the effects of possible leakage past the rotor rear air seal, the effects of inserting instruments in each row of stator blades and in the first row of outlet guide vanes, and the effects of changing the temperature and the pressure of the inlet air. The results of the interstage surveys are also presented.

19XB COMPRESSOR

The construction of the 10-stage axial-flow compressor used in the 19XB jet-propulsion unit is similar to that of the six-stage 19B compressor described in reference 1. A photograph of the assembled 10-stage compressor with the upper half of the casing removed is shown in figure 1. A cross-sectional drawing of the compressor with the principal dimensions is given in figure 2; the path of possible air leakage past the rotor rear air seal is also shown.

The cast-aluminum inlet section and the discharge section are the same as those of the 19B compressor (reference 1). Fairing inserts were installed on the inner and outer walls after the outlet guide vanes to give a straight annular passage for the discharge measuring station. The split stator casing differs from that of the 19B compressor only in the number and spacing of the circumferential grooves for the stator-blade outer shrouds. The rotor of the 19XB compressor is constructed in four sections, whereas that of the 19B was machined from a single aluminum-alloy forging. The forward section of the 19XB rotor consists of seven blade rows machined from a single aluminum-alloy forging. The rear section, which was bolted to the aluminum section, consists of three disks, each machined from a separate steel forging. A steel sleeve pressed on the aluminum section of the rotor forms the front bearing journal. The rotor is rigidly connected to the drive shaft, which is supported by the two rear bearings. In the jet-engine installation, the rigid connection

permits the thrust of the compressor to oppose that of the turbine and thus relieves part of the load on the thrust bearing.

The design of the blading for the 19XB compressor stresses simplicity and ease of manufacture rather than any particular airfoil shape. As received from the manufacturer, all the blading of the compressor was nicked and pitted from previous running of the complete jet engine, but the tests were made with these blemishes. Most of the blade angles had been changed from their original design values by plastically deforming the metal at a point approximately one-fourth inch from the root of the blades. Table I lists the design specifications (including these deformations) for all the compressor blading.

The inlet-guide-vane diaphragm consists of 55 aluminum blades fitted and peened into circular stainless steel inner and outer shrouds. The blades have symmetrical sections and are twisted approximately 8° from the root to the tip; these blades are not tapered.

The stator blades are made of stainless steel and are fitted and peened into semicircular stainless-steel shrouds, making it possible to assemble separately each half of the casing. Each half row of blades is held in place by two locking screws. With the exception of the first stage, the stator blades have circular-arc camber lines.

The rotor blades are machined of steel and fit into cylindrical dovetail grooves in the rotor disks; the blades are held in place by stainless-steel locking keys. All of the rotor blades have a circular-arc camber line except the first and second stages at the hub. The blade fillet radius for all the rotor blades is approximately one-eighth inch.

The rotor and stator blades of the 19XB compressor had a smaller camber angle at the tip and a larger camber angle at the hub than the blades of the 19B compressor. In general, the 19XB blades were thicker, had a smaller chord length, and had slightly more twist than the blades for the 19B compressor.

APPARATUS AND INSTRUMENTATION

Apparatus

The 19XB compressor was installed in the same rig as that used to investigate the performance of the 19B model (reference 1). A drawing of the setup is shown in figure 3. The compressor was driven by a 2500-horsepower induction motor in conjunction with a magnetic

coupling and two speed-increasing gear boxes. The speed of the compressor was varied by the magnetic coupling and was held at the desired value by an electronic control system.

The refrigerated-air system supplied a limited quantity of dry air at temperatures as low as -70° F. The refrigerated air was inducted through a submerged adjustable orifice and a butterfly valve into the depression tank, which was approximately 4 feet in diameter and 6 feet in length. Three screens were located at the midsection of this tank (fig. 4) to equalize the air velocities. A wooden bellmouth was fitted to the compressor inlet to insure uniform air flow into the compressor. The air leaving the compressor was discharged into a collector through a straight annular discharge passage formed by the fairing inserts. A screen of 60-percent opening was placed at the end of the discharge section of the compressor to decrease any asymmetry in flow within the compressor caused by the two radial outlet ducts. The outlet ducts, which were attached to the collector by a flexible coupling, were connected to the laboratory altitude exhaust system. The inlet duct, the depression tank, the compressor casing, and the collector case were lagged with 1/2-inch asbestos and covered with 4 inches of hair felt to minimize external heat transfer.

Inasmuch as the performance of the compressor varies with the rate of air leakage past the rotor rear air seal, provisions were made to plug the holes in the rear housing support with copper plugs. The use of these plugs enabled the leakage to be reduced to a minimum value.

Instrumentation

The instrumentation of the compressor was similar to that of the 19B compressor. The inlet air was metered through the submerged adjustable orifice located in the inlet duct before the depression tank. The static-pressure drop across the orifice was indicated on a water manometer and all other pressures, on a common-well mercury manometer. The temperatures were measured with calibrated iron-constantan thermocouples. A bath of melting ice served as the common cold junction for all thermocouples and the thermal electromotive force was read with a sensitive potentiometer in conjunction with an external spotlight galvanometer.

Inlet-air conditions were measured in the depression tank as shown in figure 4. Because the diameter of the depression tank was large, the velocity pressure at the inlet measuring station was negligible and the total pressure was measured with two wall static-pressure taps. The inlet-air temperature was measured with three-

unshielded thermocouples; one thermocouple was located at the center of the air stream and the other two were placed 180° apart extending approximately one-sixth tank diameter into the air stream.

Conditions of the discharge air were measured halfway between the outlet guide vanes and the second bearing support struts in the annular area formed by the fairing inserts. Four wall static-pressure taps were located at the discharge measuring station 90° apart circumferentially on both the inner and outer walls. Six shielded axial-vent temperature probes were located 60° apart and spaced at the centers of equal annular area elements in a spiral pattern.

The interstage instruments were located to measure the pressure and temperature halfway between the hub and casing and also midway between the leading and trailing edges of the blades in each stator row. In each of the stator rows and in the first row of the outlet guide vanes, the total pressures were taken at three circumferential locations approximately 120° apart. These pressures were measured with straight cylindrical tubes, which had a 0.030-inch hole located one-half inch from the end of the tube. Temperature probes were located in the same axial plane and approximately 10° from each total-pressure tube.

A surge-detecting apparatus consisting of a pitot tube inserted in the outlet duct and connected to a cathode-ray oscilloscope through a pressure capsule was used to determine any unstable operating condition.

METHODS AND PROCEDURE

Presentation of data. - NACA standard sea-level conditions (29.92 in. Hg absolute and 59° F) were chosen as the basis on which all data were corrected. Adiabatic temperature-rise efficiencies η_T, total-pressure ratio P_2/P_1, and pressure coefficient ψ are plotted against the equivalent weight flow $W\sqrt{\theta}/\delta$ for various values of equivalent speed $N/\sqrt{\theta}$

These parameters can be defined as follows:

η_T adiabatic temperature-rise efficiency

$$\eta_T = \frac{T_1\left[\left(\frac{P_2}{P_1}\right)^{\frac{\gamma-1}{\gamma}} - 1\right]}{T_2 - T_1}$$

[redacted]

$\frac{P_2}{P_1}$ pressure ratio

ψ pressure coefficient $\left(\frac{2gH_{ad}}{nU_t^2}\right)$

$\frac{W\sqrt{\theta}}{\delta}$ equivalent weight flow

$\frac{N}{\sqrt{\theta}}$ equivalent compressor speed

where

g acceleration of gravity, feet per second per second

H_{ad} isentropic increase in total enthalpy per unit of mass for given pressure ratio, foot-pounds per pound

N rotor speed, rpm

n number of stages

P total pressure, pounds per square inch absolute

T total temperature, $^{\circ}R$

U_t rotor tip speed, feet per second

W weight flow, pounds per second

γ ratio of specific heats

δ ratio of inlet-air pressure to NACA standard sea-level pressure

θ ratio of inlet-air temperature to NACA standard sea-level temperature

The subscripts 1 and 2 designate the inlet and outlet stations, respectively.

The outlet total pressure used was calculated from the measured static pressure, weight flow, and temperature by the method given in reference 1.

[redacted]

Tests. - All tests were made by holding speed, inlet-air temperature, and inlet-air pressure at a set value and varying the volume flow of air from maximum (limited by laboratory refrigerated-air system) to the flow just preceding incipient surge.

With interstage instruments installed and air leakage permitted, a series of runs was conducted with an inlet-air temperature of 59° F and an inlet-air pressure of 14 inches of mercury absolute over a range of equivalent speeds from 3400 to 17,000 rpm in increments of 1700 rpm. Because instruments have an adverse effect on the performance, a series of points was run at an equivalent speed of 17,000 rpm with the instruments removed to determine the effect on the over-all performance.

With the air leakage past the rotor rear air seal eliminated, a series of points with interstage instrumentation were run at equivalent speeds of 8500 to 17,000 rpm with an inlet-air temperature of 59° F and an inlet-air pressure of 14 inches of mercury absolute to determine the effect of leakage. This series was repeated for three equivalent speeds (13,600, 15,300, and 17,000 rpm), but with inlet conditions of -59° F and 6.5 inches of mercury absolute to give a comparison of performance with two inlet conditions.

A summary of the operating conditions is given in the following table:

Equivalent speed, $N/\sqrt{\theta}$ (rpm)	Inlet-air pressure, P_1 (in. Hg absolute)	Inlet-air temperature, T_1 (°F)	Remarks
3,400-17,000	14	59	Instruments and leakage
17,000	14	59	No instruments and leakage
8,500-17,000	14	59	Instruments and no leakage
13,600-17,000	6.5	-59	Instruments and no leakage

The precision with which all measurements were made is estimated to be within the following limits:

Temperature, °F	±0.5
Pressure, inches of mercury	±0.02
Weight flow, percent	±1.0
Compressor speed, percent	±0.5

Several possible sources of error may have affected the final results: (a) discharge measurements taken in the wakes of the outlet guide vanes, (b) flow distortion caused by interstage instruments, and (c) air leakage past the rotor rear air seal, which affected weight flow, pressure, temperature, and surge characteristics of the compressor and caused the results to be somewhat unreliable.

RESULTS AND DISCUSSION

All values of speed and weight flow given in the following discussion are corrected to NACA sea-level conditions. The results obtained from the runs with interstage instruments installed and air leakage permitted are presented as the basic over-all performance data. The run with the interstage instruments removed enabled the effects of the instruments to be evaluated and the runs with the leakage path blocked enabled the effects of leakage to be discussed. The results of the interstage measurements permitted the effectiveness of each stage to be determined.

Compressor performance. - The performance of the compressor is shown in figure 5 over a range of equivalent speeds from 3400 to 17,000 rpm in increments of 1700 rpm with interstage instruments installed and with air leakage permitted to pass the rotor rear air seal. The inlet conditions of temperature and pressure were 59° F and 14 inches of mercury absolute, respectively. The peak efficiency increased from 0.64 at 3400 rpm to a maximum value of 0.75 at 15,300 rpm and then dropped to 0.72 at 17,000 rpm where data may not have been taken near enough to the surge point. Some difficulty was experienced in detecting the exact surge point of the compressor, particularly at the high speeds, because the surge-detecting apparatus was sensitive to all disturbances and because extreme caution was taken not to surge the compressor violently. The peak pressure ratio was increased from 1.08 to 3.72 from equivalent speeds of 3400 to 17,000 rpm, respectively. The peak pressure coefficient was approximately constant at 0.26 up to 17,000 rpm where it dropped slightly. The maximum weight flow at the design speed was approximately 10 percent higher than the design value of 30 pounds per second. At an equivalent speed of 13,600 rpm, the peak pressure ratio apparently is low but the temperature-rise efficiency has nearly reached the peak value. The data for this performance curve may not have been taken sufficiently near the surge point. At the design speed, the pressure ratio of the 19XB compressor was observed to be higher and the temperature-rise efficiency slightly lower than that obtained from the 19B compressor (reference 1). An explanation for the lower temperature-rise efficiency in the 19XB investigation than in the

19B investigation is that the peak pressure ratio may not have been obtained. Different amounts of leakage in the two compressors may also have caused a difference in efficiency.

Effect of interstage instruments. - When the interstage instruments were removed, the weight flow through the compressor was increased about 2.2 percent and the peak temperature-rise efficiency about 0.03 (fig. 6) at 17,000 rpm. The difference in peak pressure ratio was small, however, which shows that the difference in efficiency is due to a change in the temperature rise. The wakes produced by the instruments increased the work done by the compressor blades and thereby increased the temperature ratio and possibly the pressure ratio. The increased pressure losses caused by the instrumentation, however, nullified the possible increase in pressure ratio.

Performance with no air leakage through rotor rear air seal. - The performance of the compressor is shown in figure 7 with the leakage past the rotor rear air seal eliminated. These runs were made with inlet-air conditions of 59° F and 14 inches of mercury absolute and over a range of equivalent speeds from 8500 to 17,000 rpm. The adiabatic temperature-rise efficiency increased from 0.69 at 8500 rpm to 0.72 at 10,200 rpm and dropped to 0.68 at 17,000 rpm. The peak pressure ratio increased from 1.61 at 8500 rpm to 3.87 at 17,000 rpm. The pressure coefficient decreased from 0.27 at 8500 rpm to 0.22 at 17,000 rpm.

A comparison of the performance of the compressor with and without leakage is made in figure 8. In general, the peak pressure ratio was lower for the investigation with leakage than for the investigation without leakage although the adiabatic temperature-rise efficiency with leakage was slightly higher at the higher speeds. The peak pressure ratio and the peak adiabatic efficiency did not occur at the same weight flow. The maximum weight flow through the compressor at 17,000 rpm was approximately 5 percent greater with leakage permitted past the rotor rear air seal than with leakage eliminated. Because the outlet guide vanes at least partly limited the air flow, a greater measured air flow would be delivered by the compressor when air was allowed to leak from the compressor ahead of the guide vanes to the atmosphere.

Comparison of performance at two inlet conditions. - The performance of the compressor is shown in figure 9 for the inlet-air conditions of -59° F and 6.5 inches of mercury absolute for the equivalent speeds of 13,600, 15,300, and 17,000 rpm. These runs were made with interstage instruments installed and with no air leakage permitted past the rotor rear air seal. The peak pressure ratio increased from 2.70 to 4.46 and the peak efficiency increased from 0.66 to 0.72 as the speed increased from 13,600 to 17,000 rpm.

[redacted]

A comparison of the performance at two inlet conditions is provided by figure 10. The weight flow through the compressor decreased with reduced inlet-air temperature and pressure and references 1, 2, and 3 indicate that this effect is due to pressure rather than to temperature. The decrease in weight flow varied from 6.0 percent at 13,600 rpm to a maximum value of 9.5 percent at 15,300 rpm and then decreased to 6.0 percent at 17,000 rpm.

At inlet conditions of -59° F and 6.5 inches of mercury absolute, the peak pressure ratio was slightly lower at 13,600 and 15,300 rpm but considerably higher at the design speed of 17,000 rpm than at inlet conditions of 59° F and 14 inches of mercury absolute. The difference in pressure ratios at the design speed is explained by the fact that the compressor was operated closer to the terminal surge point for the low-pressure tests than for the high-pressure tests. The amplitude of pressure fluctuation at a given rate of pulsation was less at 6.5 than at 14 inches of mercury absolute.

Interstage measurements. - Curves of interstage temperature and pressure through the compressor at the point of peak efficiency for the runs with no leakage permitted are shown in figures 11 and 12, respectively. The temperatures presented in figure 11 are the observed temperatures in each stage through the compressor. At the low speeds the temperature variation was irregular; the largest variation occurred in the fifth stage. The pressures are presented as the ratio of the pressure in any stage to the pressure in the preceding stage (fig. 12(a)), and also as the ratio of the pressure in any stage to the compressor-inlet pressure (fig. 12(b)).

The curves of pressure ratio across any stage were very irregular at the high speeds; the maximum pressure rise occurred across stages 3, 8, and 9 (fig. 12(a)). At the design speed the pressure ratio from the compressor inlet to the first row of the outlet guide vanes was 4.2 but the pressure drop across the two rows of guide vanes reduced the over-all pressure ratio to 3.72. A comparable drop in total pressure across the outlet guide vanes occurred at all speeds.

SUMMARY OF RESULTS

The performance data of the 19XB compressor are summarized as follows:

1. At the design speed of 17,000 rpm and with inlet conditions of 59° F and 14 inches of mercury absolute, the peak efficiency was 0.72, the peak pressure ratio was 3.72, and the maximum weight flow

was 33.8 pounds per second for the runs with interstage instruments installed and with leakage permitted past the rotor rear air seal. A maximum efficiency of 0.75 was obtained at the equivalent speed of 15,300 rpm.

2. When the interstage instruments were removed, the weight flow through the compressor was increased approximately 2.2 percent and the peak temperature-rise efficiency was increased 0.03 at the design speed. Only a slight change in pressure ratio occurred.

3. At the design speed the elimination of the air leakage past the rotor rear air seal decreased the peak adiabatic temperature-rise efficiency 0.04, decreased the weight flow 5 percent, and increased the peak pressure ratio 0.25.

4. A change in inlet conditions from 59° F and 14 inches of mercury absolute to -59° F and 6.5 inches of mercury absolute increased the peak pressure ratio at design speed 0.74 and decreased the weight flow approximately 6 percent.

5. The results of the surveys with the interstage instruments located in each stator row and the first row of outlet guide vanes indicated that some nonuniformity of blade loading existed and that a considerable loss of total pressure was occasioned by the outlet guide vanes.

Aircraft Engine Research Laboratory,
National Advisory Committee for Aeronautics,
Cleveland, Ohio.

Richard M. Downing,
Mechanical Engineer.

Harold B. Finger,
Mechanical Engineer.

Approved:

Robert O. Bullock,
Mechanical Engineer.

Oscar W. Schey,
Mechanical Engineer.

lrp

[redacted]

REFERENCES

1. Roepcke, Fay A., Burtt, Jack R., and Medeiros, Arthur A.: Performance of Westinghouse 19B Six-Stage Axial-Flow Compressor. NACA MR No. E5K07, Bur. Aero., 1945.

2. Negulici, Charles, and Billy, W. S.: Performance of Westinghouse 9.5A Six-Stage Axial-Flow Compressor. NACA MR No. E5L07, Bur, Aero., 1945.

3. Sinnette, John T., Jr., Schey, Oscar W., and King, J. Austin: Performance of NACA Eight-Stage Axial-Flow Compressor Designed on the Basis of Airfoil Theory. NACA ACR No. E4H18, 1944.

[redacted]

TABLE I - DESIGN DATA FOR 19XB AXIAL-FLOW COMPRESSOR BLADES

NATIONAL ADVISORY COMMITTEE FOR AERONAUTICS

Blade row	Blade length (in.)		Camber angle (deg)		Blade thickness (percent chord)		Chord length (in.)		Number of blades	Stagger angle (deg)		Leading-edge radius (in.)		Trailing-edge radius (in.)		Camber-line radius (in.)	
	Leading edge	Trailing edge	Casing	Hub	Casing	Hub	Casing	Hub		Casing	Hub	Casing	Hub	Casing	Hub	Casing	Hub
I.G.V.[a]	3.325	3.325	42.0	32.0	10.5	10.5	1.000	1.000	55	23.00	16.00	0.037	0.037	0.005	0.005	1.395	1.814
1R	3.310	3.157	12.7	0	9.0	12.0	.998	1.223	23	38.30	26.65	.010	.016	.005	.005	4.509	0
1S	3.156	3.031	12.1	0	12.0	12.0	1.040	1.048	22	38.85	27.72	.014	.014	.005	.005	4.934	0
2R	3.003	2.853	11.5	0	9.0	12.0	1.020	1.223	24	39.39	28.79	.010	.016	.005	.005	5.090	0
2S	2.852	2.766	12.6	24.2	12.0	12.0	.660	.820	38	40.15	29.95	.017	.021	.005	.005	3.008	1.970
3R	2.730	2.616	12.1	24.2	9.5	12.5	.840	1.014	32	39.80	30.10	.017	.027	.005	.005	3.985	2.419
3S	2.619	2.533	12.6	24.2	12.0	12.0	.660	.826	40	40.55	32.25	.017	.021	.005	.005	3.008	1.970
4R	2.499	2.387	13.1	24.2	9.5	12.5	.855	1.014	32	41.30	33.40	.017	.027	.005	.005	3.747	2.419
4S	2.393	2.307	12.6	24.2	12.0	12.0	.660	.826	40	40.95	34.16	.017	.021	.005	.005	3.008	1.970
5R	2.271	2.161	13.8	24.2	9.5	12.5	.870	1.014	34	42.26	34.91	.017	.027	.005	.005	3.622	2.419
5S	2.168	2.104	14.1	23.5	12.0	12.0	.597	.660	52	43.28	35.59	.016	.016	.005	.005	2.433	1.621
6R	2.080	2.003	13.7	23.5	10.0	14.0	.760	.828	43	43.32	36.27	.016	.032	.005	.005	3.185	2.032
6S	2.009	1.945	14.1	23.5	12.0	12.0	.597	.660	56	43.68	36.93	.016	.016	.005	.005	2.433	1.621
7R	1.922	1.845	14.5	23.5	10.0	14.0	.767	.828	45	44.05	37.60	.016	.032	.005	.005	3.039	2.032
7S	1.850	1.786	14.1	23.5	12.0	12.0	.597	.660	58	44.08	38.26	.016	.016	.005	.005	2.433	1.621
8R	1.766	1.689	15.1	23.5	10.0	14.0	.770	.828	47	45.01	38.91	.016	.032	.005	.005	2.930	2.032
8S	1.698	1.646	15.5	33.5	12.0	12.0	.500	.662	76	45.75	39.95	.013	.017	.005	.005	1.853	1.149
9R	1.623	1.559	15.35	43.6	10.0	12.0	.496	.702	78	46.35	34.90	.011	.020	.005	.005	1.856	.945
9S	1.568	1.516	15.5	33.5	12.0	12.0	.500	.662	76	46.35	41.50	.013	.017	.005	.005	1.853	1.149
10R	1.492	1.460	16.7	43.6	10.0	12.0	.510	.702	78	46.70	35.80	.011	.020	.008	.008	1.756	.945
O.G.V.1[b]	1.477	1.477	25.0	25.0	9.0	9.0	.600	.600	98	47.50	47.50	.012	.012	.001	.001	1.386	1.386
O.G.V.2[c]	1.489	1.605	51.7	51.7	9.0	9.0	.701	.701	98	15.15	15.15	.014	.014	.001	.001	.805	.805

[a]Inlet guide vanes
[b]First row of outlet guide vanes
[c]Second row of outlet guide vanes

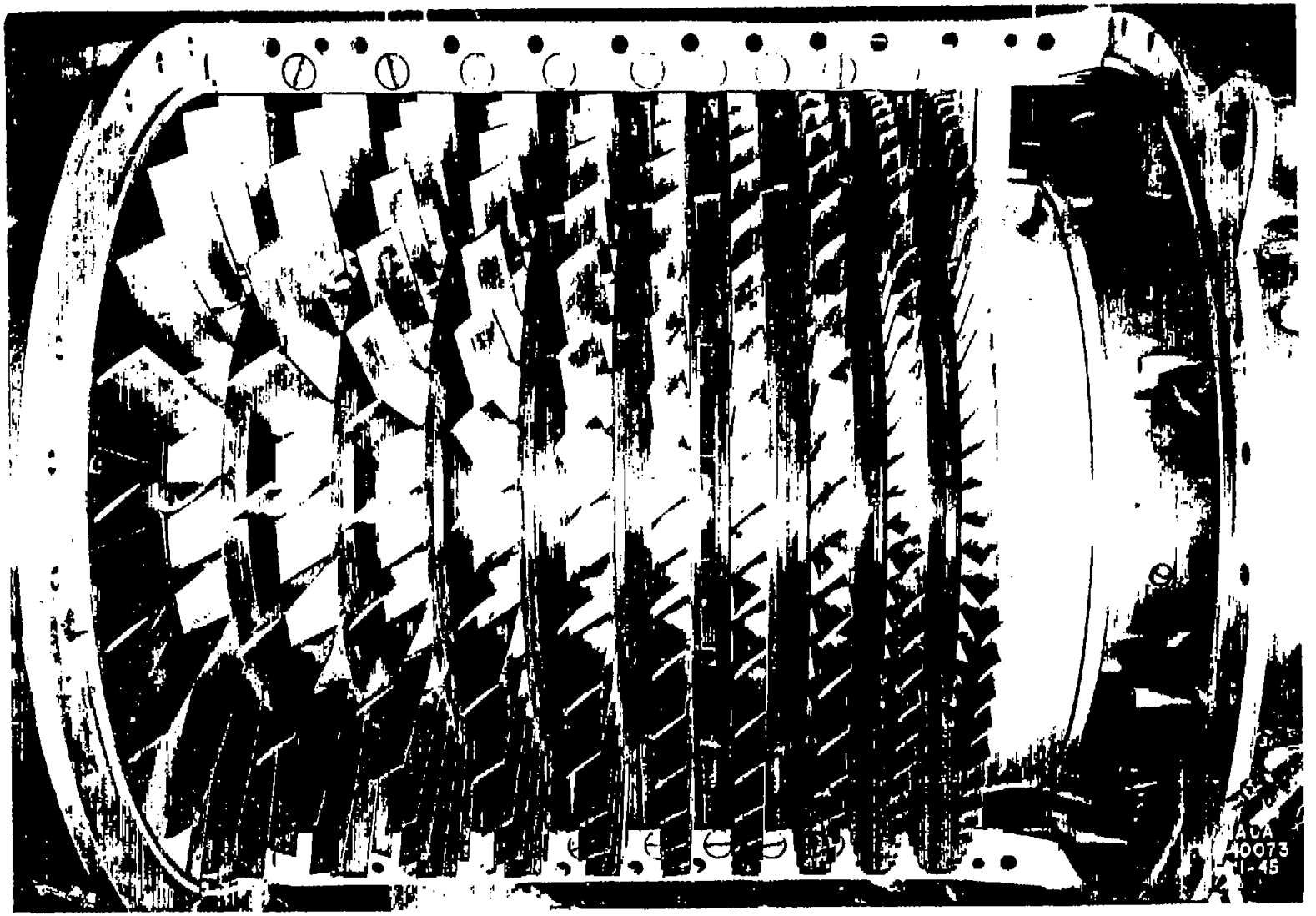

Figure 1. - Photograph of 19XB axial-flow compressor with top half of casing removed.

252+577

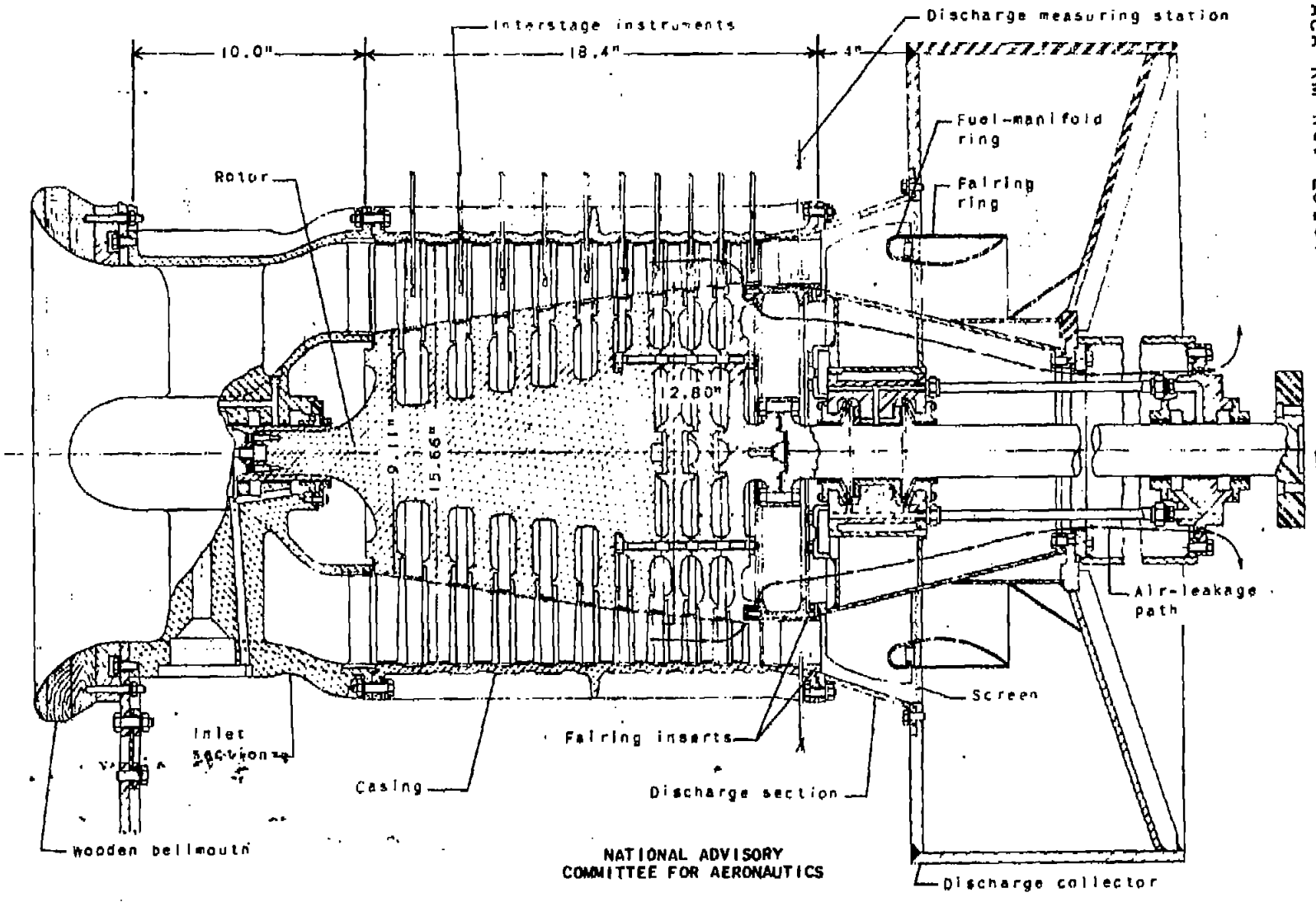

Figure 2. - Sectional view of 19XB compressor mounted with discharge collector.

Fig. 2

179+333

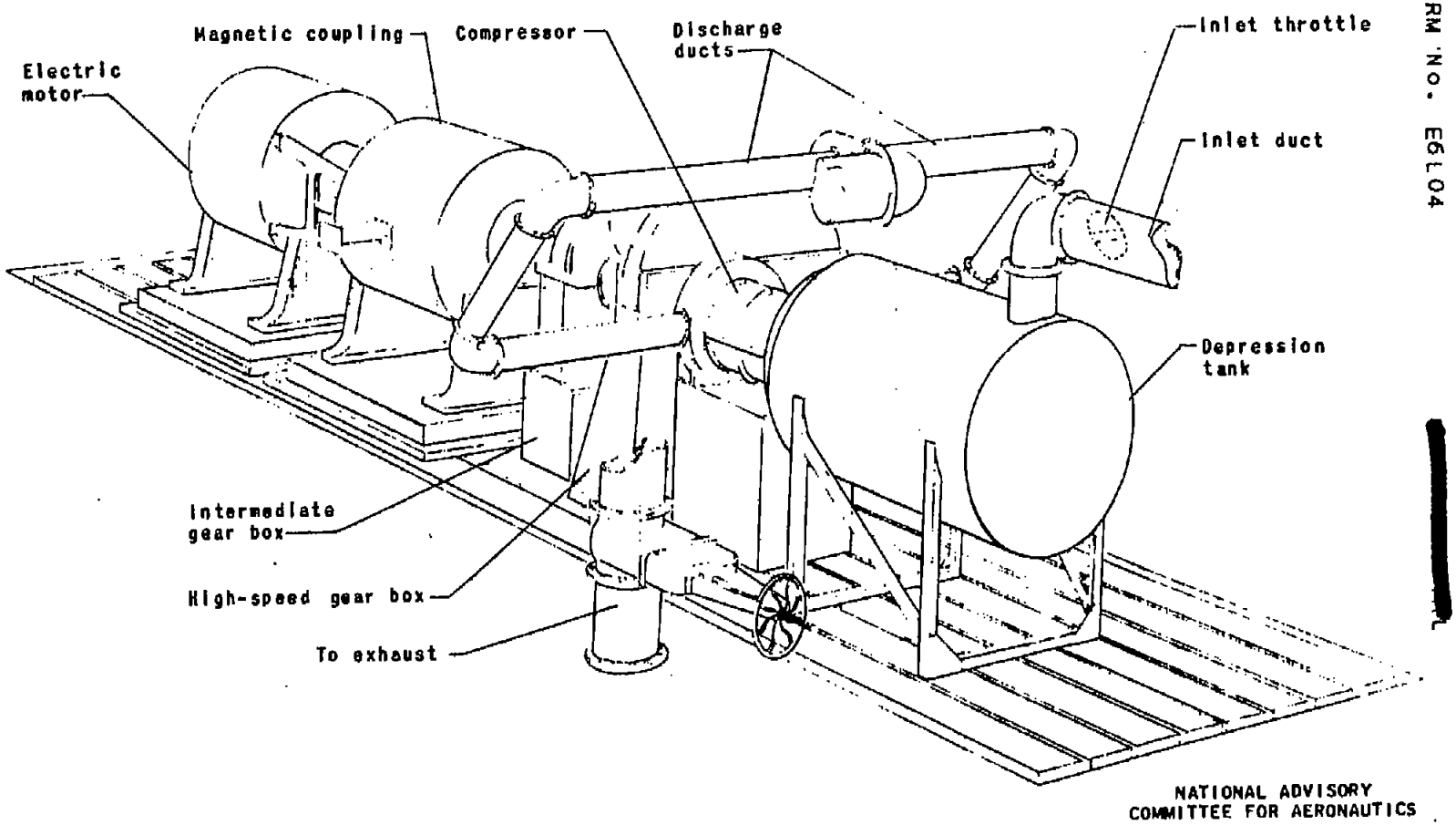

Figure 3. - Setup of 19XB axial-flow compressor with lagging removed.

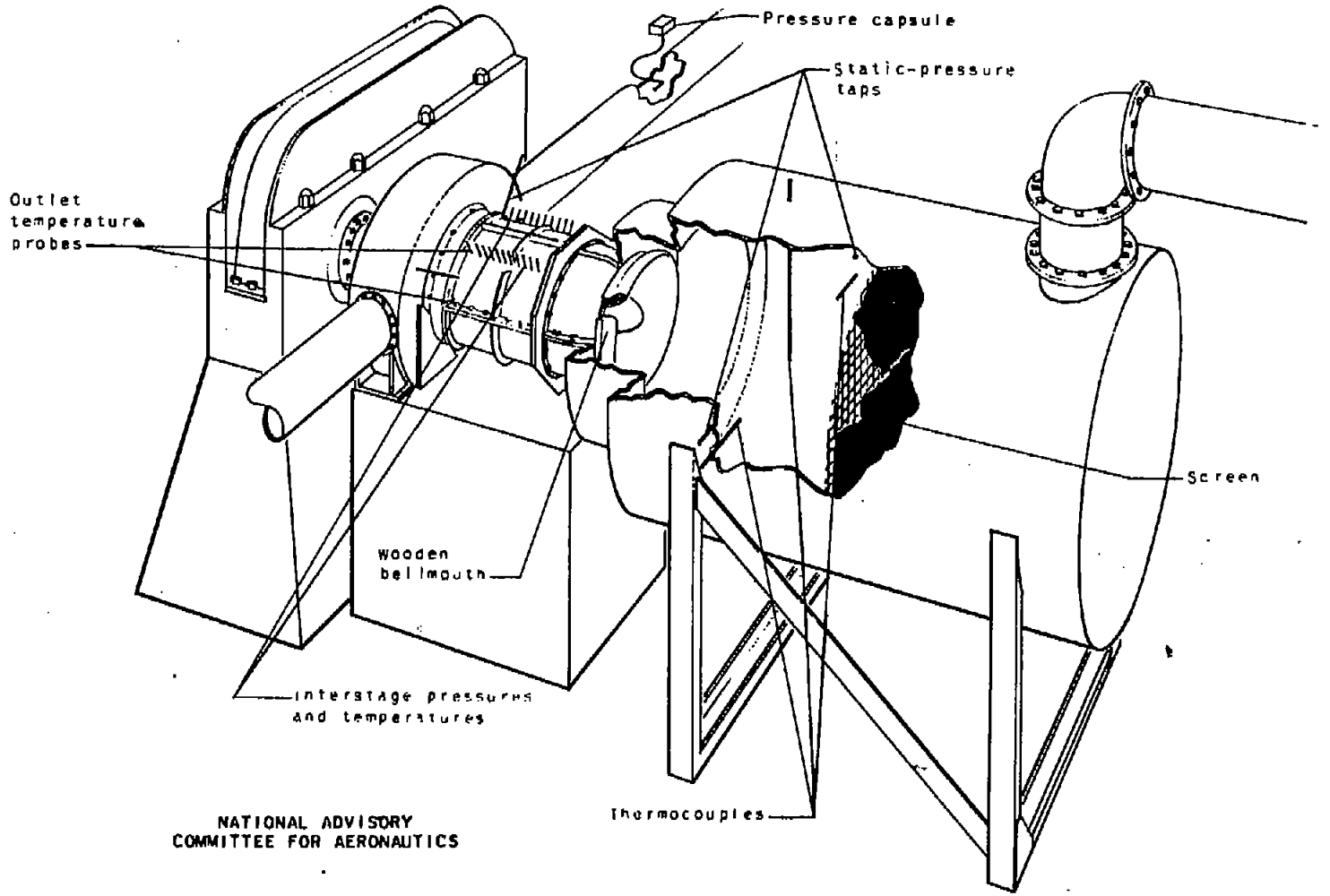

Figure 4. - Instrumentation of 19X8 axial-flow compressor with lagging removed.

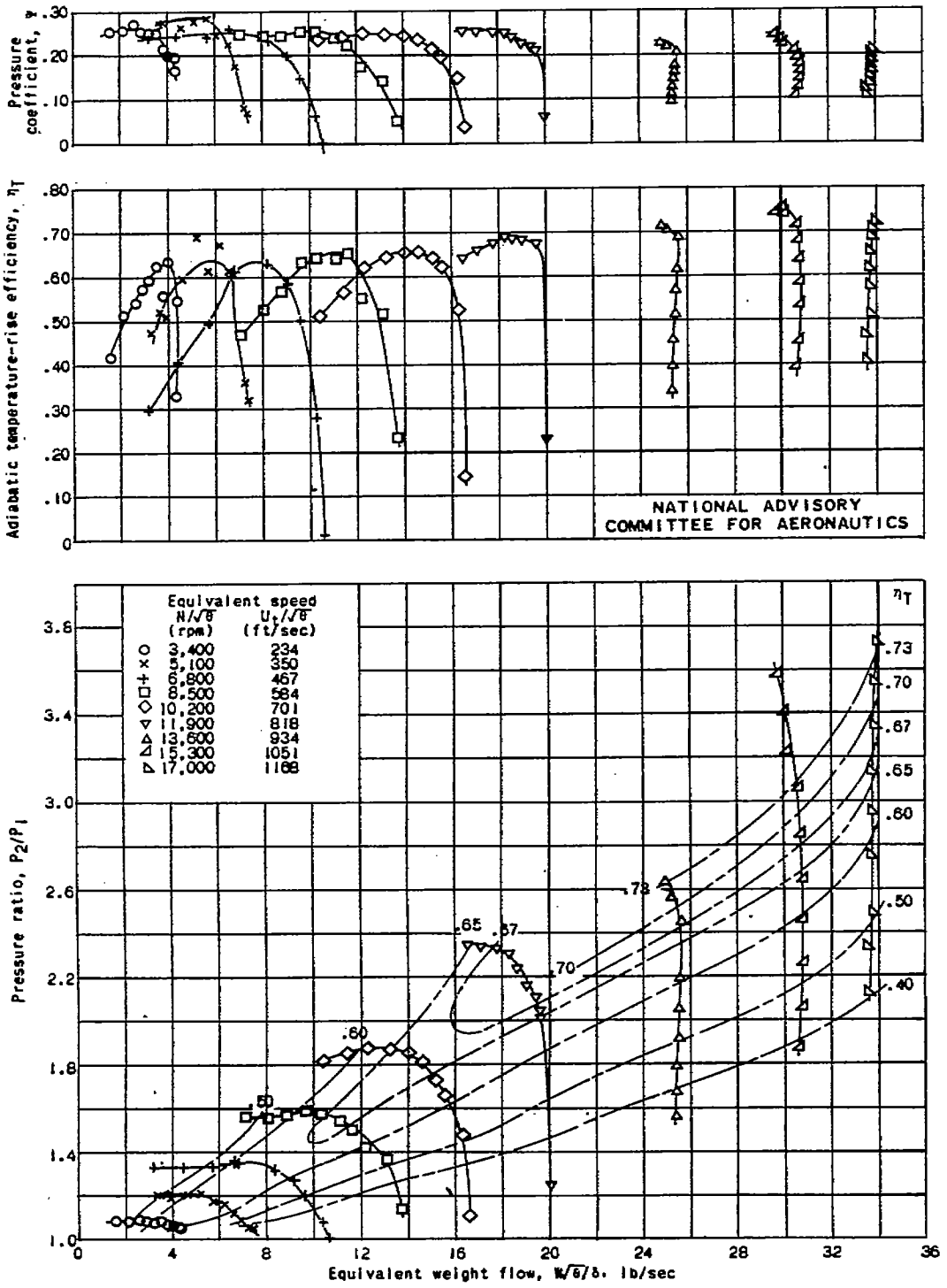

Figure 5. - Performance characteristics of 19XB axial-flow compressor for inlet-air conditions of 59° F and 14 inches of mercury absolute with air leakage past rotor rear air seal and with interstage instruments installed.

[redacted]

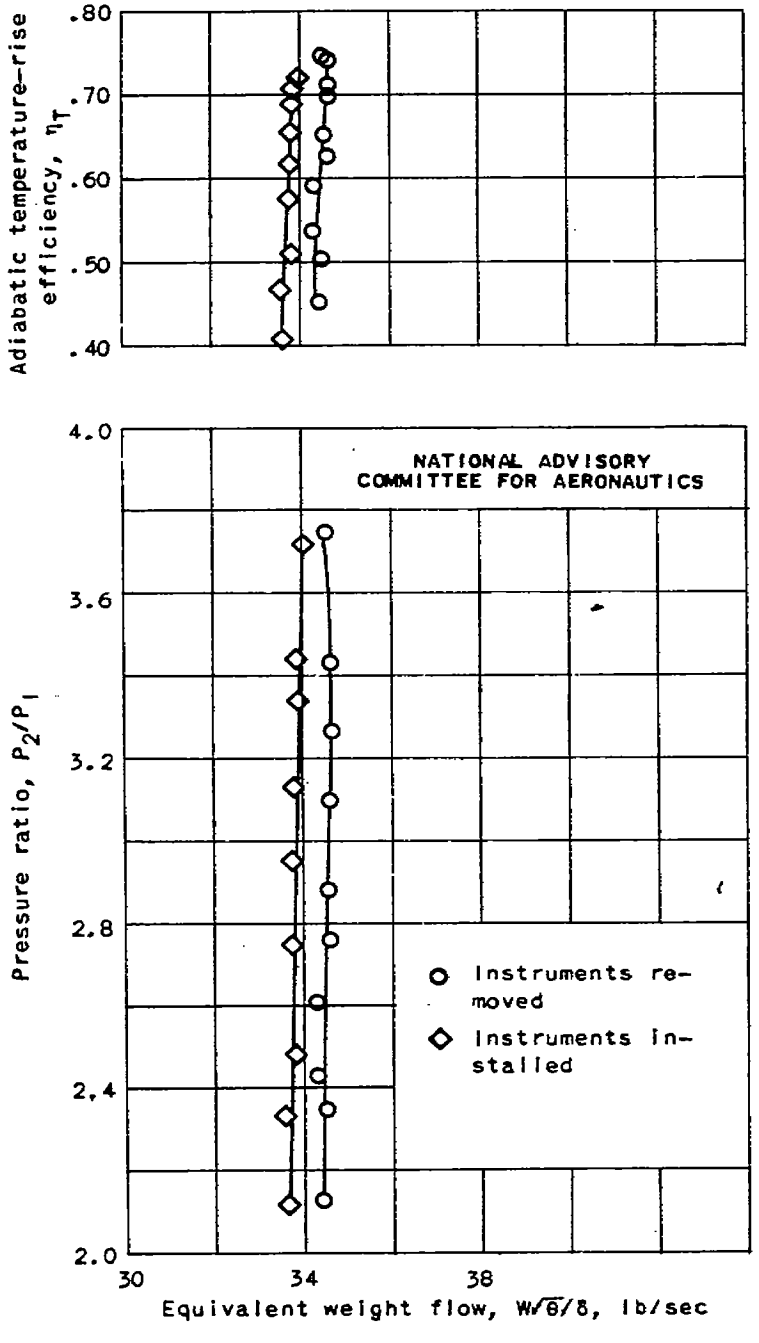

Figure 6. – Effect of interstage instruments on performance of 19X8 axial-flow compressor at 17,000 rpm at inlet-air conditions of 59° F and 14 inches of mercury absolute with air leakage past rotor rear air seal.

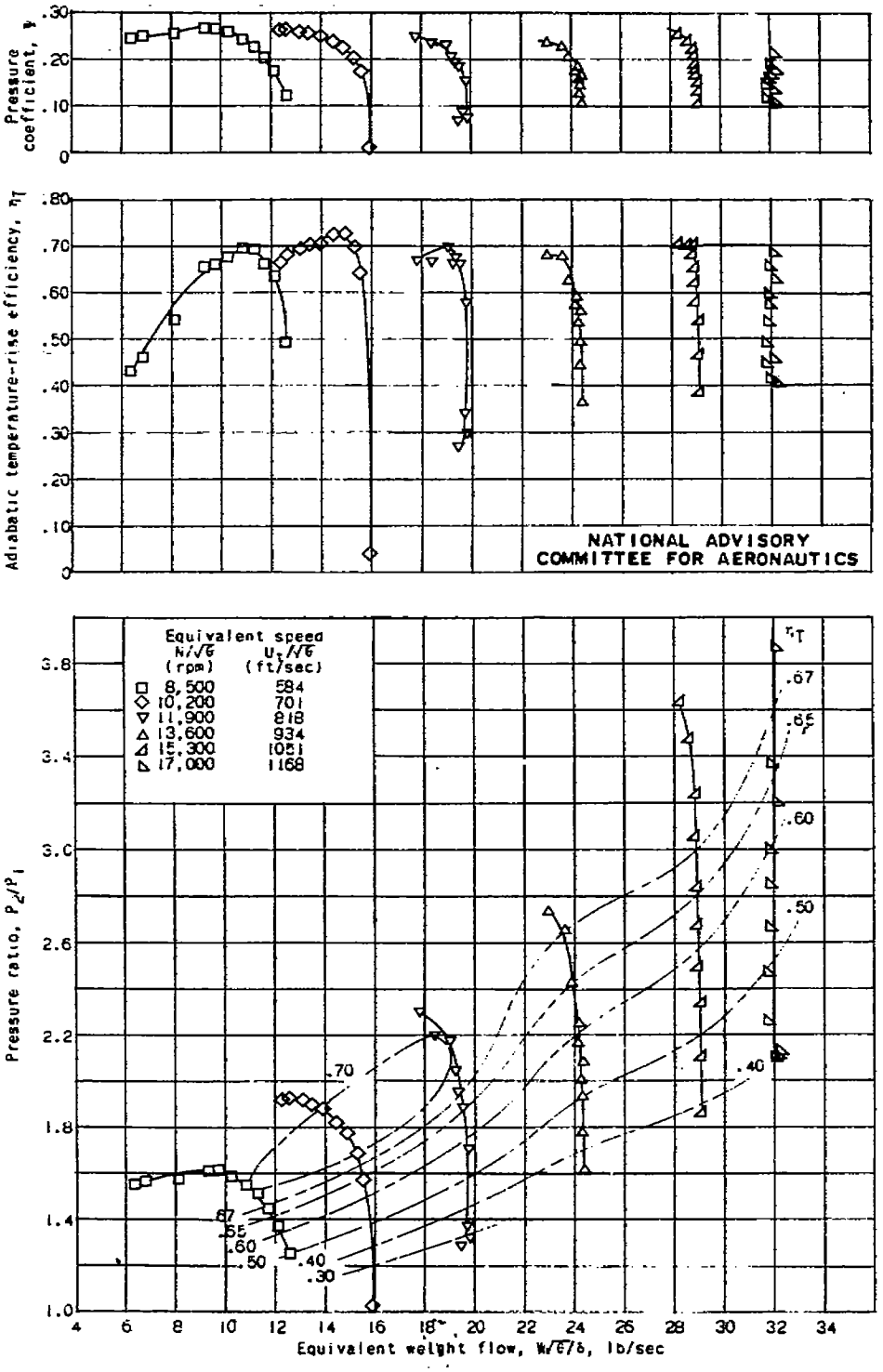

Figure 7. - Performance characteristics of 13XB axial-flow compressor for inlet-air conditions of 59° F and 14 inches of mercury absolute with air leakage past rotor rear air seal eliminated and with interstage instruments installed.

[redacted]

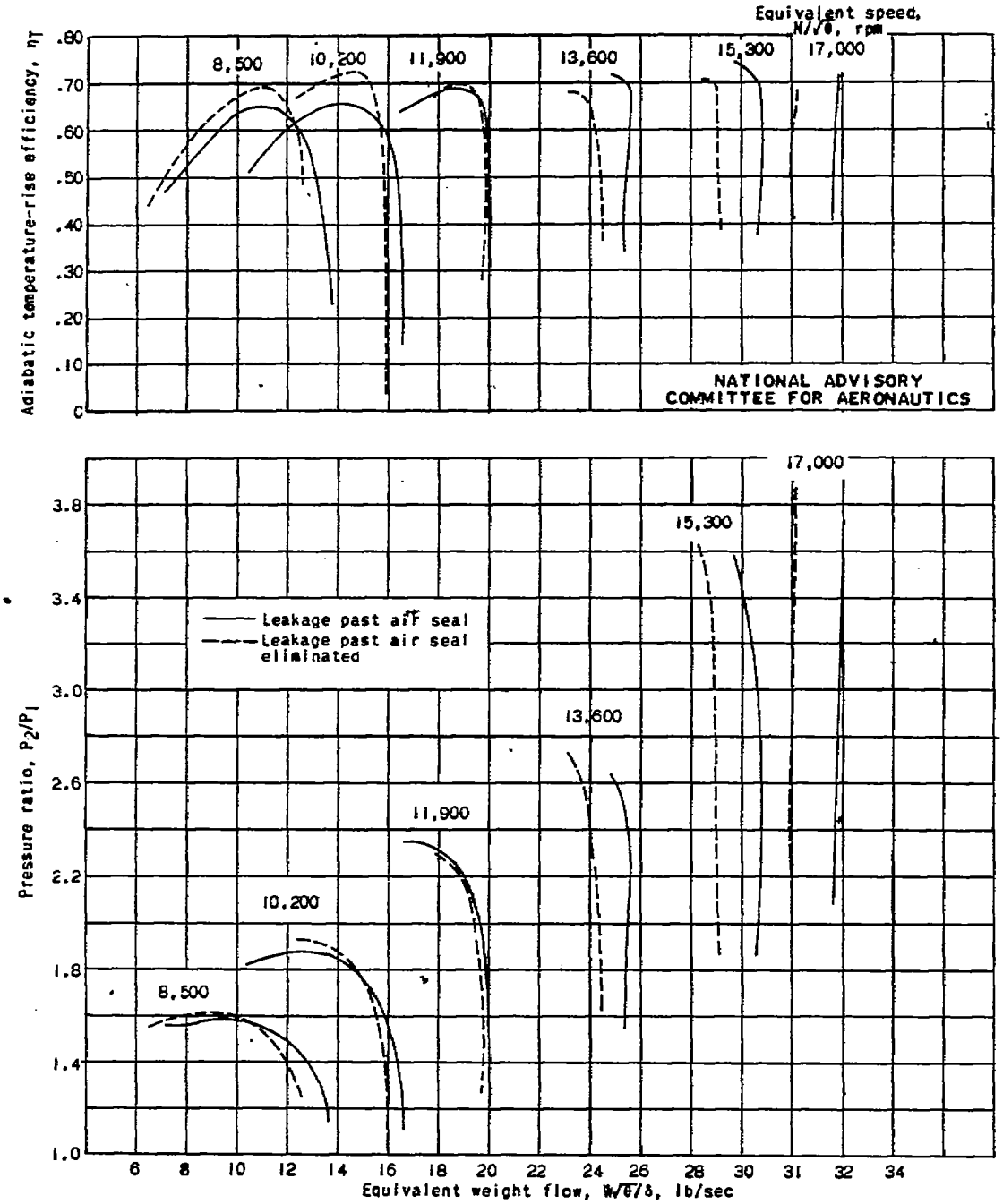

Figure 8. - Effect of leakage past rotor rear air seal on performance of 19XB axial-flow compressor with inlet-air conditions of 59° F and 14 inches of mercury absolute and with interstage instruments installed.

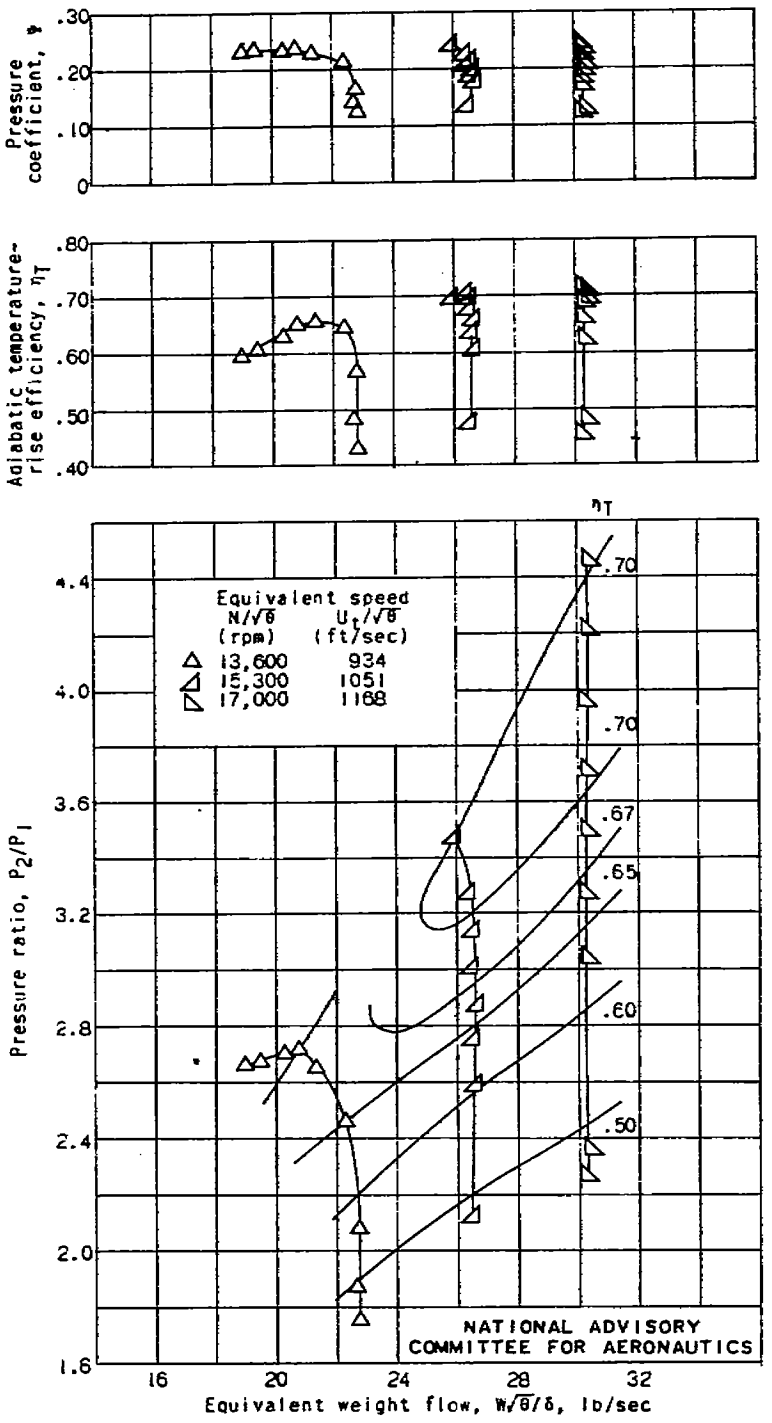

Figure 9. - Performance characteristics of 19XB axial-flow compressor for inlet-air conditions of -59° F and 6.5 inches of mercury absolute with leakage past rotor rear air seal eliminated and with interstage instruments installed.

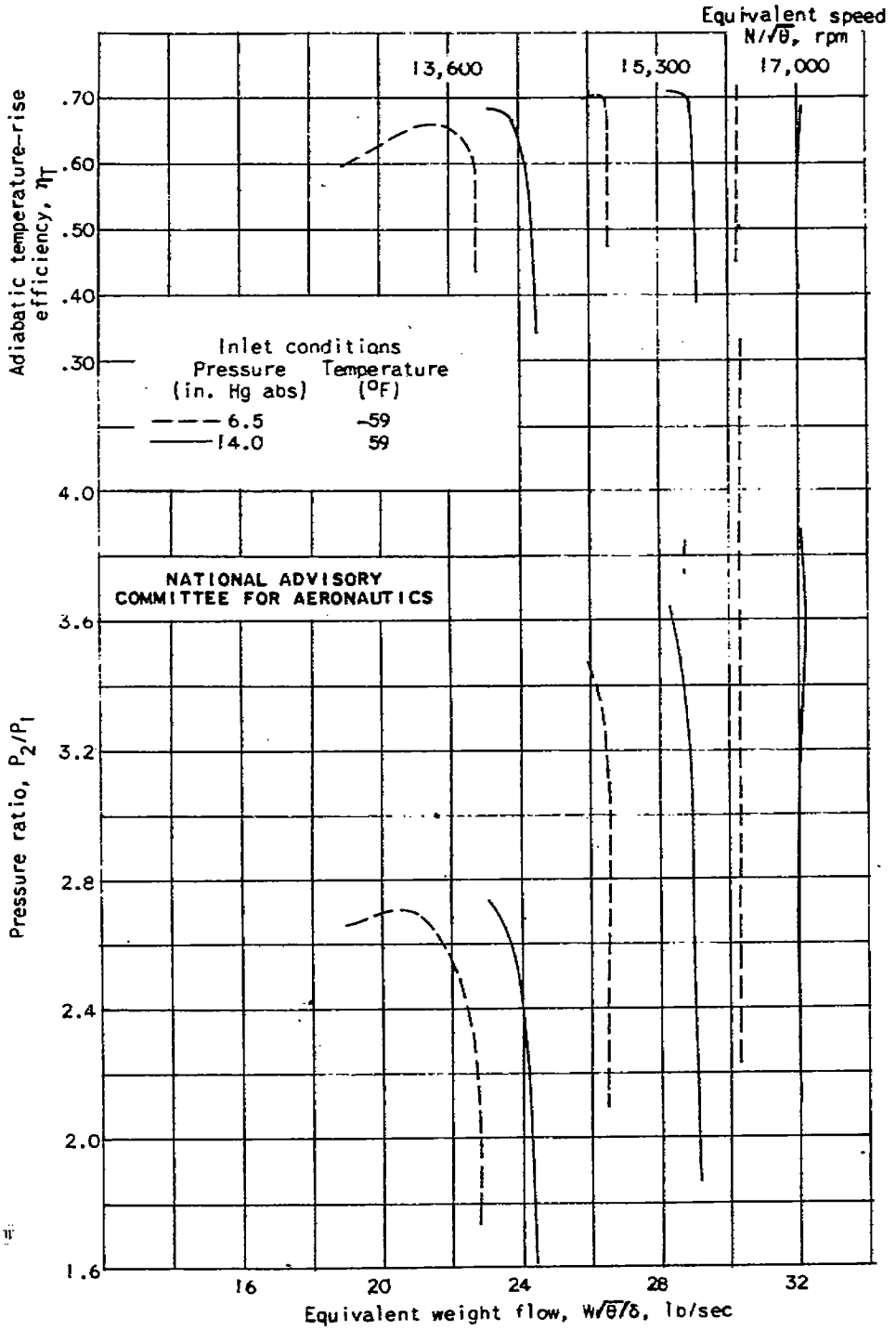

Figure 10. - Effect of inlet conditions on the performance characteristics of 19XB axial-flow compressor with air leakage past rotor rear air seal eliminated and with interstage instruments installed.

[redacted]

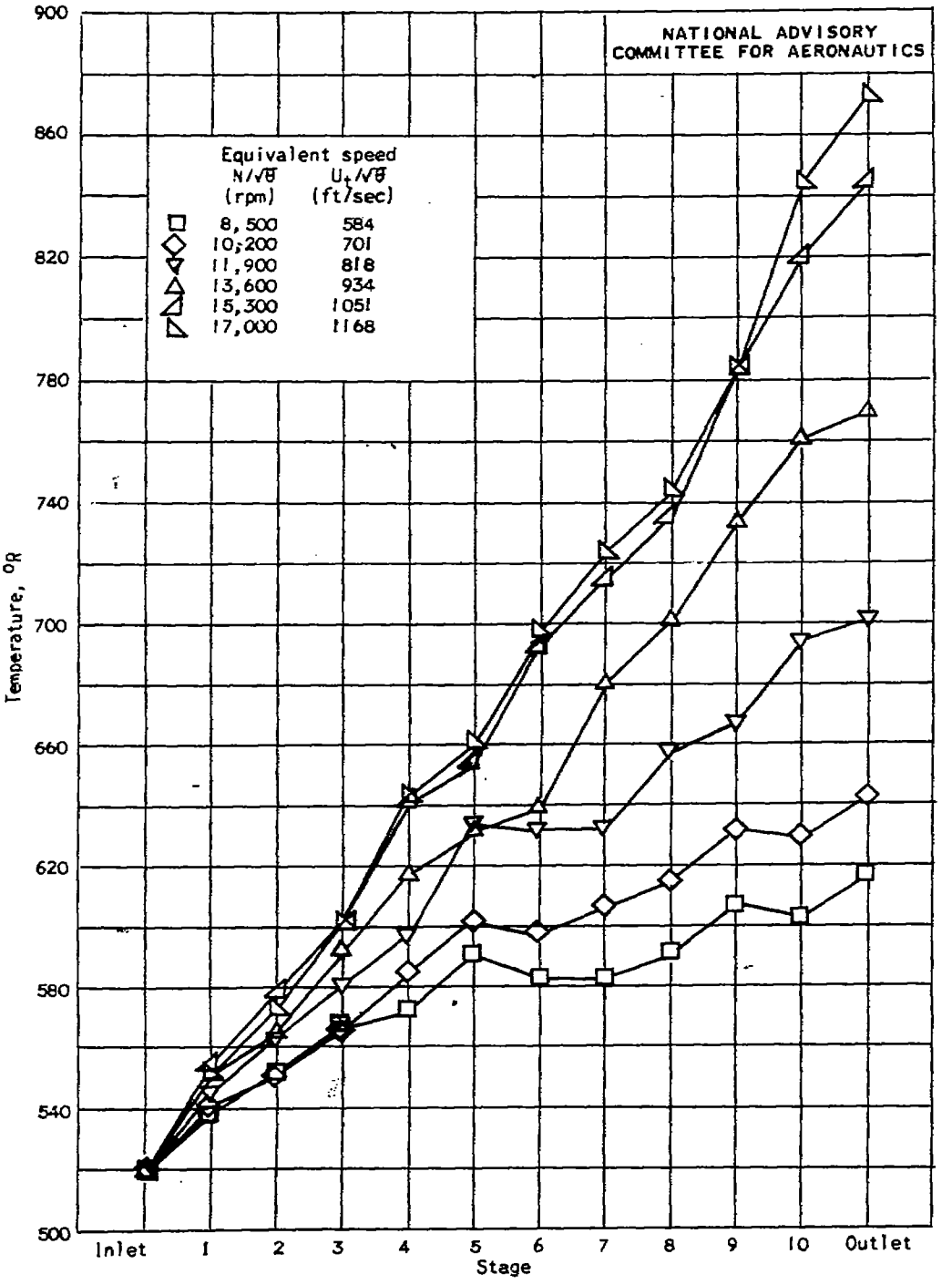

Figure 11. - Temperatures at various stages through the 19XB axial-flow compressor for inlet conditions of 59° F and 14 inches of mercury absolute at the point of peak efficiency with leakage past the rotor rear air seal eliminated.

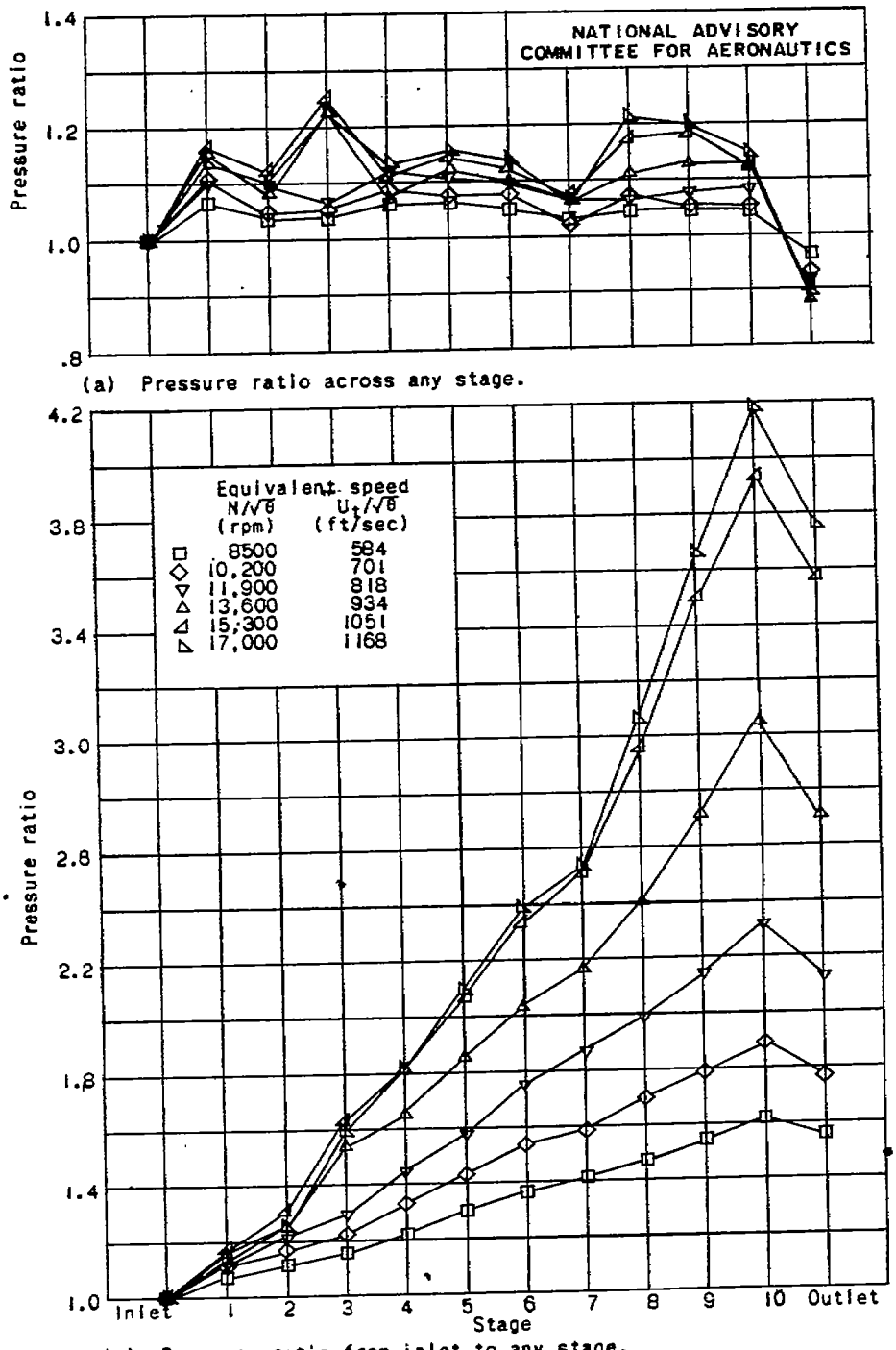

(a) Pressure ratio across any stage.

(b) Pressure ratio from inlet to any stage.

Figure 12. - Total-pressure ratios at various stages through the 19X8 axial-flow compressor for inlet conditions of 59° F and 14 inches of mercury absolute at the point of peak efficiency with leakage past the rotor rear air seal eliminated.

[redacted]

Author 12)

Engines, Jet - Westinghouse 19 X B

Compressors, Axial-flow

(10-stage)

Westinghouse 19 X B

Axial (10-stage)

[redacted]

Engines - Westinghouse 19 X B

Jet

[redacted]